Feasibility experiments for electron ripple injection on current drive experiment-upgrade

W. Choe,[a] M. Ono, Y. S. Hwang,[a] and C. S. Chang[b]
Plasma Physics Laboratory, Princeton University, Princeton, New Jersey 08543

(Received 29 July 1997; accepted 25 November 1997)

In search of a method to generate a radial electric field in tokamak plasmas, an experimental study has been performed to investigate the possibility of inducing radial electrical current. An external coil array has been used to create a local magnetic ripple well and the electron cyclotron resonance heating (ECH) has been used to trap some electrons that will then be subject to rapid vertical drifts into the plasma. Using a simplified experimental arrangement with only a toroidal magnetic field, an ECH-driven radial electrical current has been observed. The ECH-driven elecron temperature anisotropy, which is necessary for ripple trapping and electron drifts, has been determined by several different methods. The perpendicular temperature can be shown to be as large as 11 times the parallel temperature, which should yield a significant amount of ripple trapping and radial current. © *1998 American Institute of Physics.* [S1070-664X(98)01303-2]

I. INTRODUCTION

Improvement of plasma confinement is an important research topic for tokamak plasmas, and, if successful, it could lead to more economical tokamak reactors. According to the present H-mode (high-confinement mode) threshold power scaling, the required auxiliary power to induce the H mode in future high-density, high-temperature devices such as the International Thermonuclear Experimental Reactor (ITER),[1] is too high. This problem, however, can be resolved if a way is found to lower the threshold power in a direct and controlled fashion. From recent confinement studies, a radial electric field (E_r) is found to play a crucial role in inducing an improved confinement regime. This suggests that if a large enough E_r is generated and controlled by external means, we can then have a versatile ''knob'' to control plasma transport.

Since the discovery of the H-mode, several experiments have demonstrated that the H mode can be triggered by externally injecting radial current using various different types of material electrodes. Motivated by these results, an emissive limiter biasing experiment[2] was performed on the Continuous Current Tokamak (CCT).[3] The key feature of this experiment, which made it unique from other plasma biasing experiments, was the use of an emissive cathode as a limiter. In this experiment, the H mode was induced at a limiter bias voltage with an emissive limiter that was three times lower than was the case with a cold limiter. The result suggests that the performance of limiter/divertor biasing experiments can be significantly improved via electron injection. However, direct material contact with high-density and high-temperature plasmas is undesirable. Therefore, a novel electron ripple injection (ERI) technique has been proposed. The motivation for this work is a development of a nonintrusive method to produce E_r at the plasma edge, without introducing any material electrode, which therefore can be directly applied to future reactor-grade devices.

As a detailed discussion on the principle of ERI is found in Refs. 4 and 5, it is summarized briefly as follows. A pair of magnets is used to provide local bending of poloidal magnetic fields (referred to as the ''generation of magnetic field ripple''), resulting in the creation of a magnetic ''well'' localized both toroidally and poloidally (Fig. 1) along the field line. As they follow magnetic field lines, some electrons at the plasma edge, whose perpendicular energy is larger than parallel energy brought about by electron cyclotron resonance heating (ECH), can be trapped in the magnetic well. While being trapped, these electrons will move toward the plasma center via ∇B and curvature drifts if the ripple region is placed appropriately. Since the ∇B and curvature drift direction depends upon the toroidal field direction, the electron injector should be placed either at the top or bottom of a torus in order for the electron drift direction to point toward the plasma center. The ripple-trapped electrons will eventually be detrapped due to a combination of collisions and the decreasing ripple field. Since these penetrating electrons accumulate at the flux surfaces where they are detrapped from the ripple region, the net effect is to charge the plasma flux surfaces negatively. This results in a buildup of an electrostatic potential, i.e., E_r is created from the edge toward the plasma interior with a scale length of the penetration distance.

To substantiate further the feasibility of the ERI concept, a supporting theoretical study was performed.[5] A semianalytic analysis was done to estimate the ECH-induced temperature anisotropy of the electrons, which is directly related to the ripple-trapping fraction. In addition, a numerical Monte Carlo guiding-center simulation was performed to study the generation of E_r by the ∇B injection of the ripple-trapped electrons. The result suggests that about 10 MW of

[a]Permanent address: Korea Advanced Institute of Science and Technology, Taejon, Korea.
[b]Also at the Korea Advanced Institute of Science and Technology and New York University.

 © 1998 American Institute of Physics

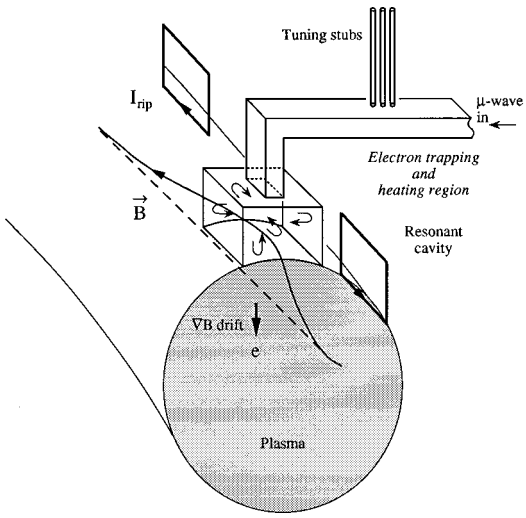

FIG. 1. Schematic of an electron ripple injector.

ECH power in ITER may be able to create a large enough radial electric field for an H-mode transition.

Concurrent with the theoretical work, experiments were performed on the Current Drive Experiment-Upgrade (CDX-U)[6] device to elucidate the underlying physics of ERI (i.e., the creation of a magnetic well; ripple trapping and ECH; and electron drifts). In Sec. II, we describe a simple experimental setup, using a microwave resonant cavity in the presence of toroidal magnetic field, for the experimental confirmation of charged particle drifts. In Sec. III, magnetic field line bending produced by the application of magnetic ripple fields is studied by monitoring the trajectories of electrons emitted from an electron source. The measured excursion length of a field line is compared with the numerical results. In Sec. IV we describe the measurement of the electron current caused by ripple trapping and ECH. As the electron temperature anisotropy generated by ECH is important in the ERI concept for providing electron injection, the determination of the electron temperature anisotropy is investigated with different methods in Sec. V. A summary is given in Sec. VI.

II. ELECTRON DRIFT EXPERIMENT

Since the vertical electron drift motion induced by ECH is the main transport mechanism for energetic electrons to generate a radial electric field in ERI, an experimental confirmation of these ECH-induced drifts would be important. To demonstrate this, a copper cube with 20 cm sides and a wall thickness 0.3 mm was installed inside the CDX-U vacuum chamber, as shown in Fig. 2. The cube had an opening to allow the access of pulsed 2.45 GHz microwaves for the ECH production of plasma. This opening was connected directly to a type WG-283 waveguide, and there was no other plasma source. Two opposite walls of the copper box consisted of 14 copper strips, insulated from one another and from the rest of the box. A toroidal field was the only magnetic field applied for this experiment, and the mounting of the copper box in relation to the toroidal field and the strips is shown in Fig. 2(b). The strips constitute faces perpendicular to the toroidal field, while their long dimension was orineted in the direction of $\nabla|B|$, which is in the radial direction for the toroidal chamber. Thus, the drift directions, parallel to the vectors $\pm\mathbf{B}\times\nabla|B|$, are normal to the face of the microwave port.

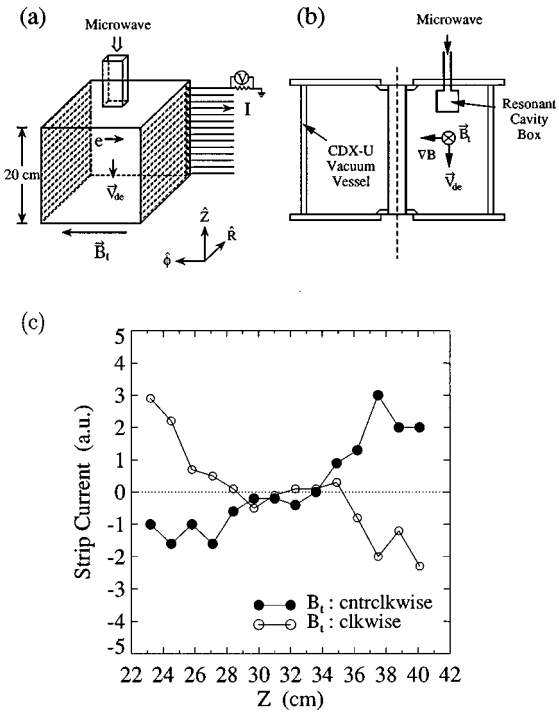

FIG. 2. Experimental arrangement implemented to study charged particle drifts. (a) Resonant cavity to observe vertical drifts. Fourteen copper strips are aligned horizontally and perpendicularly to the toroidal magnetic field. (b) Location of the cavity inside the CDX-U vacuum chamber. (c) Measured strip current distribution showing particle drifts. With a toroidal magnetic field counterclockwise in plan view (closed circles), the electron drift direction is downward, and vice versa for ions. With a reversed toroidal field (open circles), the behavior is opposite.

Wire connections to each strip were brought out via vacuum feedthroughs and grounded (i.e., returned to the chamber wall) through a resistor. The voltage across the resistor was measured during the pulse, thus yielding the current to each strip.

Figure 2(c) shows the measured strip current distribution. Closed circles indicate strip currents with toroidal fields in the counterclockwise sense looking downward at the toroidal plane of the experimental setup. With the toroidal field in the counterclockwise sense, vertical drifts generate a charge separation such that electrons move downward and ions move upward. As shown in the figure, the net strip currents are negative (electron dominant) for the lower strips and positive (ion dominant) for the upper strips, as expected. As seen in the open circles, the pattern is reversed (or clockwise) with a reversed toroidal field, since the drift direction depends on the toroidal field direction. This simple experiment demonstrates the effectiveness of ECH in producing a vertical electron drift.

III. MAGNETIC FIELD LINE BENDING EXPERIMENT

In order to study the effects of ripple fields on the electron behavior with good controllability, a pair of ripple coils

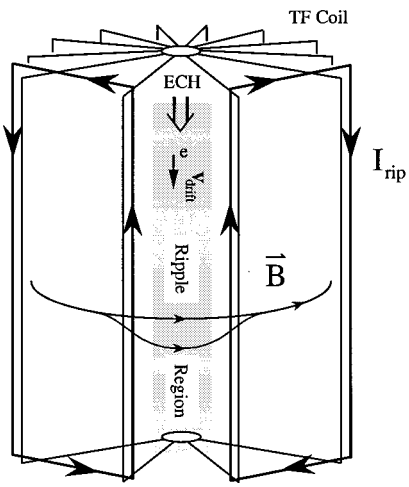

FIG. 3. A pair of ripple coils with respect to rectangular-shaped CDX-U toroidal field coils. The ripple effect is expected global in the vertical direction.

was prepared by winding wires around two rectangular-shaped CDX-U toroidal field coils, as shown in Fig. 3. In this particular configuration, the field ripple is local in the toroidal sense, but ''global'' in the vertical direction. Several field lines with ripple strengths for this configuration are depicted in Fig. 4, which shows that field lines are pulled out in major radius, creating a toroidally local magnetic well. Hereafter, all of the experiments were performed in the presence of only a toroidal field with and without ripple fields.

In this experiment, a simple setup [Fig. 5(a)] was devised to verify how the addition of a ripple field bends toroidal field lines. A tungsten filament with a hot spot of 1 mm in diameter and 8 mm in length was installed along the major radius, at the center of the ripple region, to generate an electron ring in a hydrogen gas. The radial excursion of the electron ring was measured using a Langmuir probe placed 180°

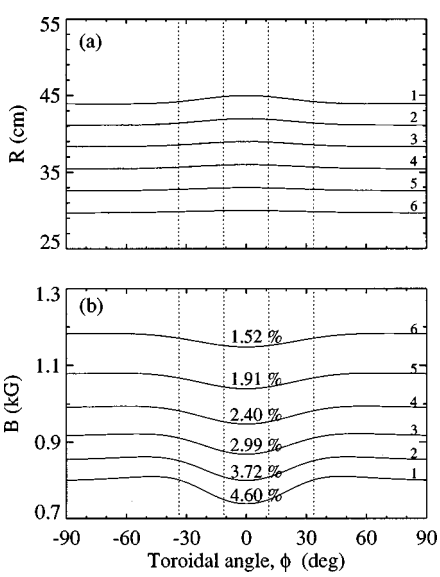

FIG. 4. Magnetic field lines with ripple fields generated by coils as in Fig. 3 added to a toroidal field. Here $B_0=0.11$ T $R_0=0.35$ m, $I_{rip}=5$ kA turn. The numbering is for indicating each field line.

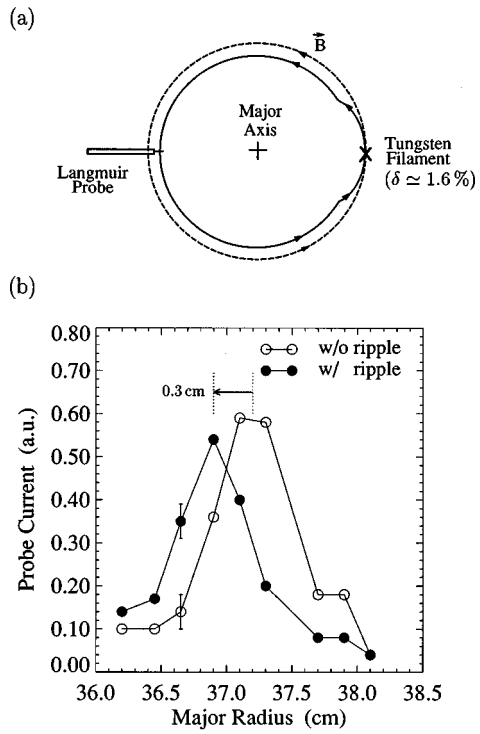

FIG. 5. (a) Plan view of the experimental setup for studying field line bending. Electrons emitted from a tungsten filament move along field lines. A Langmuir probe is used to detect electrons. (b) Radial profile of the probe current. The shift of peak indicates major-radial bending of field lines. Here $\delta=(B_{max}-B_{min})/(B_{max}+B_{min})\times 100=1.6\%$ at the electron source position.

toroidally away from the electron source. The open circles in Fig. 5(b) denote the case with only a toroidal field applied, and closed circles with a ripple field added to the toroidal field. In the case with a ripple field, the ripple strength at the electron source position was $\delta\simeq 1.6\%$, where $\delta(\%)\equiv(B_{max}-B_{min})/(B_{max}+B_{min})\times 100$. As the ripple field is added, the peak shifts toward a smaller major radius. The role of the added ripple field is to bend a field line such that it bulges outward in the ripple region, as compared to the case with only a toroidal field, as shown in Fig. 5(a). In such a field line configuration, electrons emitted from the source along the field line move inward in major radius as they move out of the ripple region, to reach the probe tip located where the ripple effect is negligible. The measured radial excursion is about 0.3 cm, which is consistent with the numerically calculated value, as shown by the arrow in Fig. 5(b) at this ripple strength.

IV. OBSERVATION OF RADIAL CURRENTS

Figure 6 depicts an experimental setup where a hydrogen plasma was generated and heated (ECH) by 2 kW of 2.45 GHz microwaves in the presence of a toroidal field plus a ripple field. Two copper limiters, placed inside and outside the ripple region, respectively, were installed in such a way that they encompass the whole radial extent of the CDX-U device [Fig. 6(b)]. The collecting edges of the limiters were located at the midplane of the chamber to ensure that no vertical field would be present at the collecting limiter edges. In the absence of a vertical field, the only vertical drift is due

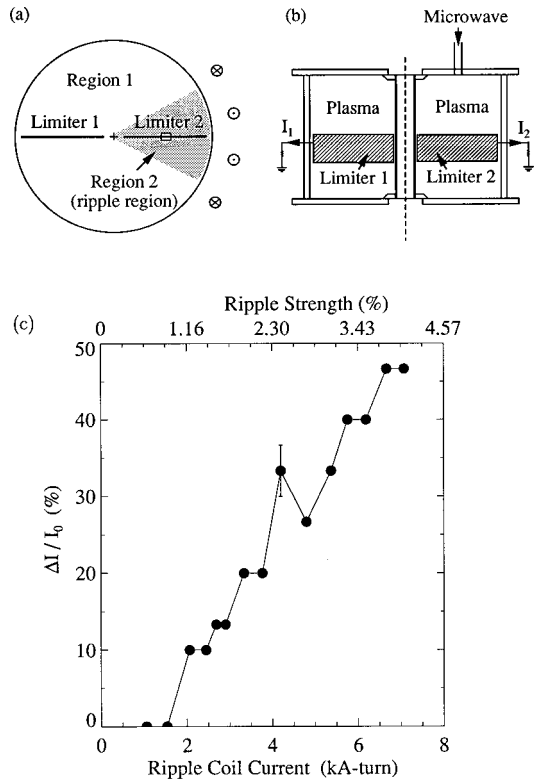

FIG. 6. Arrangement to study ripple trapping and ECH. (a) Plan view with ripple coil positions depicted, and (b) side view of CDX-U. Copper limiters implemented on the midplane cover a whole radial extent of the chamber. Not drawn to scale. (c) The difference between the limiter currents at the inside and outside ripple regions. I_0 is the limiter current in the absence of ripple fields.

to the ∇B and curvature drifts. Since the limiters collect electrons drifting downward by these drifts, the role of a ripple field and ECH can be investigated by simply comparing the two limiter currents. As the electrons are heated by ECH, preferential heating of the perpendicular temperature $T_\perp$ causes more and more particles to be trapped in the ripple region. The larger number of trapped particles and higher $T_\perp$ causes more electrons to drift downward in the ripple region. Thus, one would expect an increased current with ECH for the limiter that is located in the ripple region.

The abscissa of Fig. 6(c) denotes the ripple strength at the electron cyclotron resonance location, where the microwaves are introduced. The ordinate denotes the difference between the inside and outside limiter currents, normalized to the current without the ripple field. As is seen in the figure, the limiter current inside the ripple region increases by as much as 50% as the ripple strength is increased. This enhanced limiter current is the radial current generated by ERI through ripple trapping and ECH. The measured current will be compared with a model calculation in the next section. The measured limiter currents will also be used in determining the electron temperature anisotropy, and thus, the perpendicular temperature of the resonant electrons.

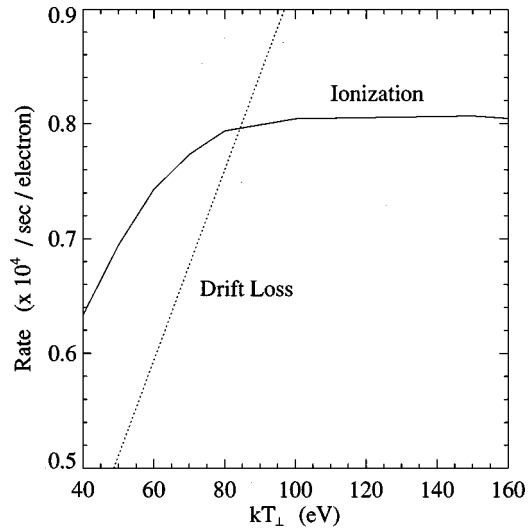

FIG. 7. A plot of the ionization source rate versus the drift loss rate of electrons as a function of the electron temperature. The two terms balance at 85 eV, giving $T_\perp / T_\parallel \simeq 11$ with $kT_\parallel \simeq 8$ eV. This is the upper bound for $T_\perp$. The rates are divided by electron density.

V. DETERMINATION OF ECH-INDUCED, RIPPLE-TRAPPED ELECTRON TEMPERATURE ANISOTROPY

The temperature anisotropy of resonant electrons driven by ECH plays a crucial role in ripple trapping and ripple transport. The measurement of the temperature anisotropy is difficult with conventional methods due to the low-density, low-temperature, and very small electron Larmor radius of the plasma. The parallel temperature $T_\parallel$, however, can be measured using a Langmuir probe. One can infer some temperature anisotropy from the probe data (although not accurately), as we discuss later in this section. The electron temperature anisotropy described in this section was determined by several different methods: particle balance, limiter current measurement, density measurement, Langmuir probe analysis, and theoretical modeling.

First, since the main loss mechanism of the experiment described in Fig. 6 is the drift loss, a simple evaluation of the particle balance between the drift loss rate and ionization source rate is useful to obtain the electron energy distribution. The drift loss rate can be expressed as $[n_w(v_d)_w + n_b(v_d)_b]L$, where the first and the second terms are the resonant electron (w) and the background (b) electron contribution, respectively. Here, n_w, n_b are the resonant and background electron densities, $(v_d)_w$, $(v_d)_b$ are the drift speed of the resonant and background electrons, respectively, and L is the vertical plasma scale length. The drift loss rate is linearly proportional to the electron temperature, since $v_d \propto T$. Noting that the plasma source is solely from ionization by electrons, the ionization rate can be given by $(n_w\langle\sigma v\rangle_w + n_b\langle\sigma v\rangle_b)n_{\mathrm{H}}$, where n_{H} is the hydrogen neutral density and $\langle\sigma v\rangle$ is the Maxwellian-averaged ionization rate coefficient. Using the $\langle\sigma v\rangle$ value from Ref. 7, the loss and source rates are compared in Fig. 7, which indicates that the two terms balance at $\kappa T_\perp \simeq 85$ eV. This simple particle balance suggests that the plasma will experience serious ''pump out''

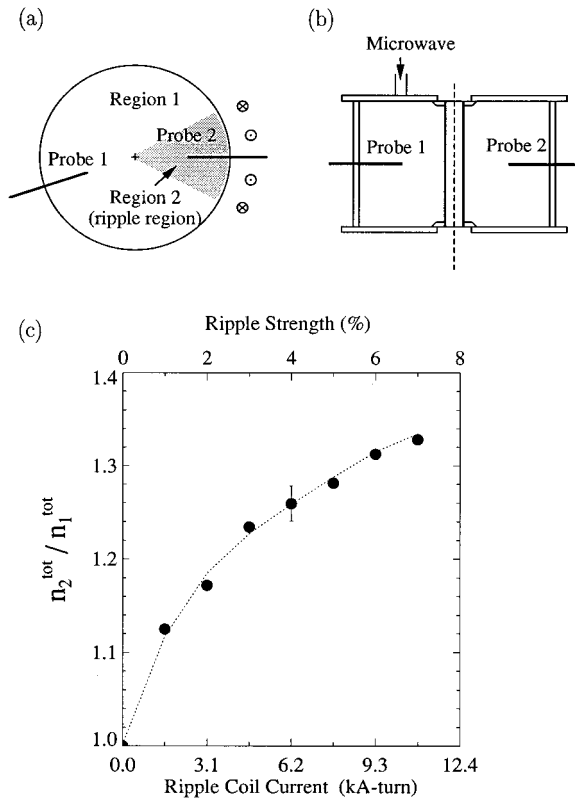

FIG. 8. Arrangement for the determination of temperature anisotropy by electron density measurements: (a) Plan view and (b) side view of the CDX-U vacuum chamber. (c) shows the total density ratio in two regions (inside and outside ripple region) at various ripple strengths.

when the electrons are heated above $kT_\perp \simeq 85$ eV. Since the experiment was conducted without the ''pump out,'' the upper bound for $kT_\perp$ can be set to be 85 eV. This results in $T_\perp / T_\parallel \leqslant 11$ using $kT_\parallel$ of 8 eV (measured by a Langmuir probe, which will be described in the following paragraphs). For the resonant electron fraction, $n_w/(n_b+n_w)=0.4$ was used, based on density measurements with the third method described below.

Second, the perpendicular temperature of warm electrons can also be estimated from the limiter current measurement (Fig. 6), because the limiter current is due to electron drifts. All the electrons that drift down would then be collected by the limiter, since it covers the whole radial extent of the vacuum chamber. The limiter current can be expressed as

$$I_{\lim} \simeq [n_w(v_d)_w + n_b(v_d)_b] \frac{eV_{\rm pl}}{L},$$

where $V_{\rm pl}$ is the plasma volume in the ripple region, and L is the scale length of the electron drift. $(v_d)_w$ is linearly proportional to $kT_\perp$. Using the measured current $I_{\lim} \simeq 1$ A, background electron temperature $kT_b = 8$ eV, $B = 0.087$ T, $R = 0.35$ m, $L \leqslant 0.35$ m, $V_{\rm pl} \simeq 0.04$ m^3, $kT_\perp$ is determined to be 86 eV, with a corresponding temperature anisotropy of $\leqslant 11$.

The third method involves electron density measurements with the experimental arrangement (Fig. 8) similar to that for the limiter current measurement (Fig. 6). For the sake of simplicity, the volume of the CDX-U chamber is divided into two different regions, with *Region 1* and *Region 2* being the unperturbed and perturbed (by the ripple magnetic field) regions, respectively. A couple of Langmuir probes (one in each region) were used in this setup instead of limiters. As seen in Fig. 8(c), there is an electron density gradient between the two regions. This is attributed to ripple trapping and the temperature anisotropy driven by ECH. With the data points shown in Fig. 8(c) in hand, it is possible to estimate the warm electron temperature anisotropy in the ripple region (*Region 2*) by calculating the ratio of particle densities in the two regions in terms of magnetic well depth and temperature anisotropy.

In a relatively collisionless plasma, where collisions are not sufficiently frequent to randomize particle motions perpendicular and parallel to the magnetic field, the pressure tensor can be anisotropic. This condition is well satisfied in this experiment. With the total density n_2, we write the distribution function in *Region 2* as

$$f = f_N \exp\left[-\frac{m_e}{2kT_\parallel} \left(\frac{v_\perp^2}{s} + v_\parallel^2 \right) \right], \tag{1}$$

where

$$f_N = n_2 \Big/ \left(\frac{2\pi kT_\parallel}{m_e} \right)^{1/2} \left(\frac{2\pi ksT_\parallel}{m_e} \right).$$

$T_\parallel$ and $s(=T_\perp/T_\parallel)$ are the parallel temperature and temperature anisotropy in the peturbed (or ripple) region, respectively. In spherical coordinates, it can also be written as

$$f = f_N \exp\left(-\frac{m_e}{2kT_\parallel} \frac{v^2}{s} [1 + (s-1)\cos^2 \varphi] \right), \tag{2}$$

where $\varphi = \arctan(v_\perp / v_\parallel)$. Now consider the total density in *Region 1*, which is the nonripple region. As in a simple mirror geometry, the constants of motion in this case are the first adiabatic invariant $\mu(=m_e v_\perp^2/B)$, and the total energy w $(=m_e(v_\perp^2+v_\parallel^2)/2)$ of the particle. If the coordinates are changed from $(v_\parallel, v_\perp)$ to (w, μ), the Jacobian is $\mathscr{J} = m_e^2 v_\parallel / 2B$. With this, we can write

$$\int d^3v_2 f = \frac{2\pi}{m_e^2} \int f \frac{B_2}{v_{\parallel 2}} d\mu dw, \tag{3}$$

where $v_{\parallel 2} = \sqrt{2(w-\mu B_2)/m_e}$. Since the distribution function is constant along any particle trajectory in a collisionless plasma according to Liouville's theorem,[8] the total density in *Region 1* is

$$\begin{aligned} n_1 &= \int_{\rm whole} d^3v_1 f \\ &= \frac{2\pi}{m_e^2} \int_{\rm whole} f \frac{B_1}{v_{\parallel 1}} d\mu dw \\ &= \frac{2\pi}{m_e^2} \int_{\rm whole} f \left(\frac{B_1}{B_2} \right) \left(\frac{v_{\parallel 2}}{v_{\parallel 1}} \right) \left(\frac{B_2}{v_{\parallel 2}} \right) d\mu dw \end{aligned}$$

$$= \int_{\text{passing}} d^3 v_2 f\left(\frac{B_1}{B_2}\right)\left(\frac{v_{\parallel 2}}{v_{\parallel 1}}\right). \tag{4}$$

Equation (3) was used in the last step of obtaining Eq. (4), together with the fact that all the particles in *Region 1* are connected with only the passing particles in *Region 2*. By combining energy and μ conservation, $(v_{\parallel 2}/v_{\parallel 1})$ is obtained to be

$$\frac{v_{\parallel 2}}{v_{\parallel 1}} = \frac{\cos\varphi}{\sqrt{1-\left(\frac{B_1}{B_2}\right)\sin^2\varphi}}. \tag{5}$$

Evaluation of Eq. (4) is straightforward using the distribution function [Eq. (2)] and the trapping condition given with the magnetic fields B_1 and B_2 in the two regions. The total density in *Region 1* is then

$$n_1 = n_2 \frac{m}{1+s(m-1)},$$

where $m = B_1/B_2 = (1+\delta)/(1-\delta)$ with the ripple strength δ, and $s = T_\perp/T_\parallel$. In other words, the density ratio in the two regions can be expressed in terms of the magnetic field ratio (m) and the temperature anisotropy in *Region 2* (s) as

$$\frac{n_2}{n_1} = \frac{1+s(m-1)}{m}. \tag{6}$$

As extreme cases, Eq. (6) shows $n_2 = n_1$ for either $m=1$ (no ripple) or $s=1$ (isotropic distribution).

In practice, the densities observed in *Regions 1 and 2* consist of the cold background electron part (Maxwellian) and the warm electron part (anisotropic bi-Maxwellian), because not all the electrons are resonant with electron cyclotron waves. Denoting the subscript $b(w)$ to stand for the background (warm) part, we write

$$\begin{aligned} n_2^{\text{tot}} &= n_{2b} + n_{2w}, \\ n_2^{\text{tot}} &= n_{1b} + n_{1w}. \end{aligned} \tag{7}$$

Since the background part has an isotropic distribution, the background densities in both regions must be same and are independent of m, following from Eq. (6). Letting $n_b \equiv n_{1b} = n_{2b}$, and using Eq. (6) again for the warm part, n_b is expressed as

$$n_b = n_1^{\text{tot}} \frac{1}{s-1}\left[s - \frac{m\left(n_2^{\text{tot}}/n_1^{\text{tot}}\right)-1}{m-1}\right]. \tag{8}$$

Equation (8) suggests that the temperature anisotropy s can be determined by knowing the magnetic field ratio m and the measured total densities in both regions. Figure 9 shows a plot of Eq. (8) with a few data points from Fig. 8(c), where each curve corresponds to each data point with its own m, n_1^{tot}, and n_2^{tot}. Each curve crosses at $s \simeq 11.5$, which is the warm electron temperature anisotropy.

The fourth method for determining the temperature anisotropy is by the analysis of Langmuir probe I-V characteristics. The parallel temperature of electrons was also determined from the probe data. The analysis shows two temperatures of 8 and 39 eV, and it indicates the presence of a warm electron population. Here we consider the parallel temperature of electrons to be 8 eV, which is the same as the temperature of the cold isotropic electrons. The fact that the warm electron temperature anisotropy is lower than the value determined above can be attributed to the cylindrical geometry of the probe tip. The Larmor radius of a warm electron is comparable to the probe radius, so that the measured temperature lies between $T_\parallel$ and $T_\perp$.

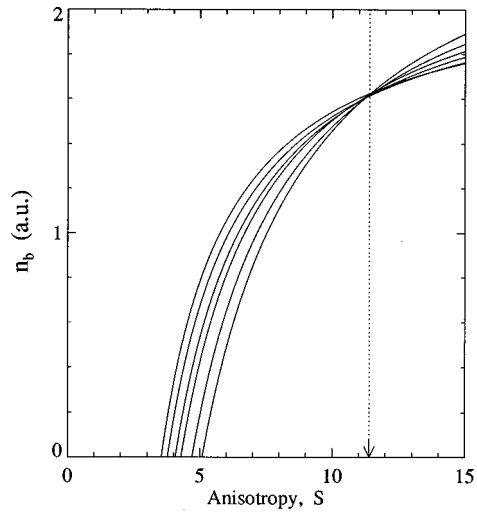

FIG. 9. Plot of Eq. (8) with several different data points. Each curve corresponds to a data point in Fig. 7(c) with each ripple strength (or m). The crossing point of curves indicates the temperature anisotropy s of about 11.

The final method, based on a semianalytic calculation, follows the procedure discussed in Refs. 5 and 9 for this experimental configuration. The temperature anisotropy at the resonance surface is plotted in Fig. 10 as a function of the normalized heating power density $d_e \equiv P_\perp/n_{2w}kT_e\nu_0$, where $P_\perp$ is the wave power density and ν_0 is the electron–ion 90° scattering frequency. Using the experimental values [$P_\perp$

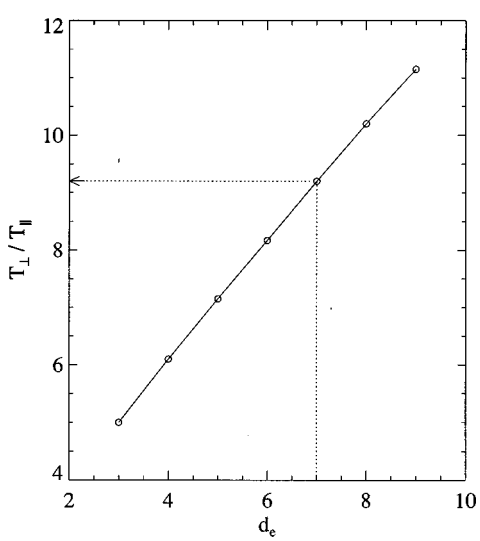

FIG. 10. Semianalytically calculated warm electron temperature anisotropy at the resonance layer. In this experimental configuration, $d_e \simeq 7$, and it results in $T_\perp/T_\parallel \simeq 9$.

$\simeq$1.7 kW/(plasma volume), $T_e \simeq 8$ eV, and $n_e \simeq 3\times 10^{16}$ m^{-3}], $d_e \simeq 7$. This results in $T_\perp / T_\parallel \simeq 9$, which is in reasonably good agreement with the other values, and lies within the experimental uncertainty.

VI. SUMMARY

A novel electron ripple injection technique to generate E_r inside the plasma to trigger the H mode has been reported recently.[5] The ultimate goal of this technique is to lower the H-mode power threshold for tokamak reactors, and to develop a versatile knob to control tokamak plasma edge transport via an externally generated E_r.

Experimental verification of the underlying physics of ERI was accomplished in the CDX-U device, utilizing microwaves for ECH and a ripple magnetic field added to the toroidal field. First, electron drifts (∇B and curvature) induced by ECH were experimentally confirmed, showing the expected directionality with respect to the magnetic field. Second, magnetic field line bending was studied using an electron emitter. Probe measurements of electrons emitted from a tungsten source showed a radial shift of the electron orbits, and thus, of the field lines due to the addition of a ripple field. The measured excursion distance is consistent with numerical calculations. Third, the currents due to electron trapping and heating were measured during ECH. The difference in the observed currents in the ripple and nonripple regions was consistent with theoretical expectations. Fourth, the resonant electron temperature anisotropy was determined by a number of different ways, and the results are summarized in Table I. The experimentally determined values agree well with the value calculated semianalytically, within experimental uncertainty.

Since both modeling and preliminary results support the feasibility of the electron ripple injection scenario, further experiments to demonstrate H-mode generation in a tokamak with this technique are warranted.

TABLE I. Electron temperature anisotropy determined by several different methods.

Method	$T_\perp / T_\parallel$
Particle balance	$\leqslant 11$
Limiter current measurement	$\leqslant 11$
Density measurement	11
Langmuir probe $I-V$	>5
Semianalytic prediction	9

ACKNOWLEDGMENTS

The authors wish to acknowledge Dr. R. Kulsrud, Dr. R. Armstrong, and Dr. R. Kaita for useful discussions. Thanks are due to M. W. Kineyko and Mr. J. Taylor for their expert technical support.

This work was supported by the United States Department of Energy under Contract No. DE-AC02-76-CH0-3073 and Grant No. DE-FG02-86-ER53223.

[1] ''ITER Conceptual Design Report,'' ITER Documentation Series, No. 18 (International Atomic Energy Agency, Vienna, 1991).
[2] W. Choe, M. Ono, D. S. Darrow, *et al.*, *Proceedings of the IAEA Technical Committee Meeting on Tokamak Plasma Biasing*, Montreal, 1992 (International Atomic Energy Agency, Vienna, 1993), p. 95.
[3] R. J. Taylor, M. L. Brown, B. D. Fried, H. Grote, J. R. Liberati, G. J. Morales, P. Pribyl, D. Darrow, and M. Ono, Phys. Rev. Lett. **63**, 2365 (1989).
[4] W. Choe, ''Feasibility study of electron injection for tokamak plasma transport control,'' Ph.D. dissertation, Princeton University, Princeton, NJ, 1996.
[5] W. Choe, M. Ono, and C. S. Chang, Nucl. Fusion **36**, 1703 (1996).
[6] Y. S. Hwang, C. B. Forest, and M. Ono, Phys. Rev. Lett. **77**, 3811 (1996).
[7] R. K. Janev, W. D. Langer, K. Evans, Jr., and D. E. Post, *Elementary Processes in Hydrogen–Helium Plasmas* (Springer-Verlag, Berlin, 1987).
[8] N. A. Krall and A. W. Trivelpiece, *Principles of Plasma Physics* (McGraw-Hill, New York, 1973).
[9] W. Choe, C. S. Chang, and M. Ono, Phys. Plasmas **2**, 2044 (1995).